RSC Advances

This article can be cited before page numbers have been issued, to do this please use: W. Luo, T. Yang, L. Su, K. Chou and X. Hou, *RSC Adv.*, 2016, DOI: 10.1039/C5RA27234C.

View Article Online
DOI: 10.1039/C5RA27234C

Journal Name

PAPER

Preparation of hexagonal BN whiskers synthesized at low temperature and its application in fabricating electrochemical nitrite sensor

E Received 00th January 20xx,
Accepted 00th January 20xx

DOI: 10.1039/x0xx00000x
www.rsc.org/

Wenpo Luo[a], Tao Yang[a], Lei Su[b], Kuo-Chih Chou[a], Xinmei Hou[a*]

Abstract. Hexagonal boron nitride (h-BN) whiskers were synthesized via the polymeric precursor method using boric acid (H_3BO_3) and melamine ($C_3H_6N_6$) as raw materials at 1073-1273K in flowing nitrogen/hydrogen (5% hydrogen). The phase and morphology of the obtained products were characterized using XRD, FTIR, SEM, TEM and BET techniques. The results show that h-BN wishers can be successfully fabricated at 1073-1273K with 0.5-3μm in diameter and 50-200μm in length. It possesses micropores and contains mesopores. Moreover, the as-prepared BN whiskers can be used as a sensing electrode for detection of nitrite (NO_2^-). Compared with other electrodes for nitrite detection, h-BN wishers electrode shows a much higher sensitivity in the wider range from 10 to 1000 μM with a detection limit of 0.089μM (10-400μM) and 0.412μM (400-6300μM) (S/N=3) respectively. The oxidation process of NO_2^- on h-BN whiskers electrode is controlled by diffusion process.

1. Introduction

Nitrite (NO_2^-) is a typical inorganic pollutant, which is highly carcinogenic to human life and aquatic animals. Moreover, nitrite is widely used as an additive and corrosion inhibitor in food. It can produce methemoglobin, which reduces the transportation of oxygen. Furthermore, nitrite reacts with various amines and amides to form N-nitrosoamines to cause stomach cancer.[1-4] It is imperative to develop detection technologies for determination of nitrite due to its high toxicity in biological systems, particularly in children. Many techniques have been developed for the in situ quantification of nitrite, including fluorescencep,[4] hotometric methods,[5] sequential injection,[6] spectrophotometry[7] and electrochemical methods.[8] Among the various detection techniques, electrochemical methods have attracted considerable attention by virtue of their fast response, simple operation, high sensitivity and excellent selectivity.[9-20] Carbon-based electrode including glass carbon, carbon paste, highly oriented pyrolytic graphite, poly(methylene blue)-modified glassy carbon electrode and basak plane pyrolytic graphite etc. have long been recognized as versatile platforms for electrocatalysis and electrochemical sensing due to their numerous advantages such as low cost, chemical inertness and wide potential window applicability in most electrolyte solutions compared to precious metal electrodes, for instance, gold, platinum, aluminium, siliver and copper etc.[21-26].

Boron nitride (BN) is well known for its excellent properties such as high hardness, high temperature stability, low dielectric constant and so forth.[27,28] These unique properties make BN a promising candidate for many applications such as refractories, lubricants, laser devices and catalyst supports.[28-31] h-BN possesses hexagonal structure with properties similar to those of graphite and have been widely fabricated to be used as ranging from organic pollutant adsorption to hydrogen storage. Till now, intensive research works have been carried out on the synthesis of BN using various methods including arc-discharge technique,[32] laser heating of h-BN at high nitrogen pressures,[33] thermal annealing of amorphous boron powder under lithium vapor in h-BN crucible[34] and CVD from borazine using NiB powders as a catalyst etc.[35–37] Few research work is reported to apply h-BN for electrochemical application.

Herein h-BN whiskers are proposed as electrode for electrochemical detection of nitrite based on its isostructural to graphite. In view of the fabrication of h-BN whiskers, a simple method is adopted using boric acid (H_3BO_3) melamine ($C_3N_6H_6$) as raw materials. By controlling the reaction temperature, h-BN can be tailored at relatively low temperature, i.e. 1073-1273K. Furthermore, the analytical performance of nitrite sensor based on h-BN whiskers was investigated using cyclic voltammetry (CV) and differential pulse voltammetry (DPV). The fabricated sensor shows high sensitivity, stability and satisfactory reproducibility.

2. Experimental

2.1 Synthesis of h-BN whiskers

Preparation of h-BN whiskers includes two steps, i.e. (1) Synthesis of the precursor using H_3BO_3 (⩾99.8 mass%) and $C_3N_6H_6$(⩾99 mass%) as raw materials; (2) Conversion of the precursor whiskers into BN whiskers under nitrogen/hydrogen (5% hydrogen). The precursor was prepared using wet chemical method. A solution containing H_3BO_3 and $C_3N_6H_6$ with the molar ratio of 3:1 was stirred for about 30 min at 363 K. Then the obtained mixture was held at room temperature for about 12 h. It was filtrated by pumping and then dried to obtain the white product as the precursor. The obtained

[a] *W. P. Luo • T. Yang • Kuo-Chih Chou • X. M. Hou (corresponding author)*
State Key Laboratory of Advanced Metallurgy, University of Science and Technology Beijing, Beijing 100083, China
E-mail: houxinmei@ustb.edu.cn
[b] *L. Su*
Research Center for Bioengineering and Sensing Technology, School of Chemistry and Biological Engineering, University of Science and Technology Beijing, Beijing 100083, China.

View Article Online
DOI: 10.1039/C5RA27234C

precursor was then slowly heated in a tube furnace to the require temperature, i.e. 1073-1273k for 3-5h in flowing nitrogen/hydrogen (5% hydrogen) and then taken out from the furnace at 973K to cool to room temperature in nitrogen. Finally the white whiskers were obtained.

2.2 Phase and microstructure characterization

The phase of the samples was examined by powder X-ray diffraction (XRD) with a TTRIII diffractometer equipped with CuKα radiation over a 2θ range from 10 to 90° (XRD, M21XVHF22, MAC Science, Yokohama, Japan). Besides, Nicolet-Nexus-670 Fourier transformation infrared spectroscopy (FTIR) with spectral scanning between 4000 and 500 cm^{-1} was also used to identify the structure of the product (FTIR; Nicolet-Nexus 670, Germany). X-ray photoelectron spectra (XPS) were recorded on an AXIS Ultra DLD X-ray photoelectron spectrometer, using non-monochromatized Mg Ka X-rays as the excitation source (XPS, AXISULTRA-DLD, Kratos, Japan). Morphology of the samples was examined by thermal field emission scanning electron microscopy (FE-SEM; ZEISS SUPRATM 55, Germany) and transmission electron microscopy (TEM, HITACHI H8100, Hitachi, Japan). Further structural characterization was observed using high resolution electron microscopy (HRTEM, JEM 2010, Joel Ltd. Japan) and selected area electron diffraction (SAED) pattern. The specific surface area (calculated using Brunauer-Emmett-Teller (BET) model) was determined from the nitrogen adsorption-desorption isotherm measured at 77K on a Quadrasorb SI-MP analyzer.

2.3 Electrochemical measurement

The work electrode was prepared by mixing h-BN whiskers and polyvinylidene fluoride (PVDF) with the mass ratio of 95:5 in N-methyl-2-pyrrolidone(NMP) to form stable slurry. Then the stable slurry was coated on a Ti sheet with the coating mass of about 3 mg (1×1cm). Finally the electrode was heated at 373K for 6 h to evaporate the solvent for electrochemical detection.

The electrochemical measurements were carried out on a CHI660D electrochemistry working station. A conventional three-electrode cell was used with a silver chloride electrode as the reference, a platinum wire as the counter and modified h-BN whiskers electrode as the working electrode. Electrochemical measurements including cyclic voltammogram (CV), linear sweep voltammetry (LSV), differential pulse voltammetry (DPV) and current-time (I-t) plot were performed in the solution of phosphate buffer (PB) containing $NaNO_2$. The scan rate was 0.1 v/s for CVs and 0.03-0.17 v/s for LSV. DPV experiments were performed with amplitude of 0.05 V, pulse width of 0.2 s and pulse period 0.5 s. All experiments were carried out at about 298K and all solutions were prepared using reagent grade chemicals in deionized water.

3. Results and discussion

3.1 Phase and microstructure characterization

Fig. S1 shows the XRD pattern of the sample obtained at different temperature. According to the XRD pattern, all the reflection peaks at the range of 10°-90° can be indexed to the (002) , (100) and (110) planes of h-BN. No impurities such as B_2O_3 can be detected. Compared with the result reported in the literature, in which h-BN whiskers were obtained at much higher temperature, 1873K,[38] the characteristic peaks are obviously broadened, indicating the crystallinity of BN is not high and BN whiskers are either in nanometer size or highly defective in structure.

FTIR spectra of the sample as shown in Fig. S2 indicate two strong characteristic peaks locating at 1381.0 and 801.0 cm^{-1}, in which the absorption band at 1381.0 cm^{-1} is identified with the B–N stretching vibrations and the absorption band at 801 cm^{-1} can be attributed to the B–N–B bending vibrations. Two broad absorption peaks at 3417.0cm^{-1} and 3182.0 cm^{-1} should be attributed to the O-H band in adsorbed water and N-H.[39,40]

The morphology of the sample obtained at 1073K was characterized using SEM and TEM (Fig. 1). The SEM image (Figs. 1a-c) shows the typical BN whiskers appear to possess nonuniform morphology. The diameters of h-BN whiskers are about 0.5-3μm and the lengths are ranging from 200 to 500 mm. HRTEM image (Fig. 1e-f) shows the crystallinity of the obtained product is not well, which accords well with the XRD result. These can act as the effective adsorption site and allow the strong adsorption of the target ions, which leads to improved sensitivity.

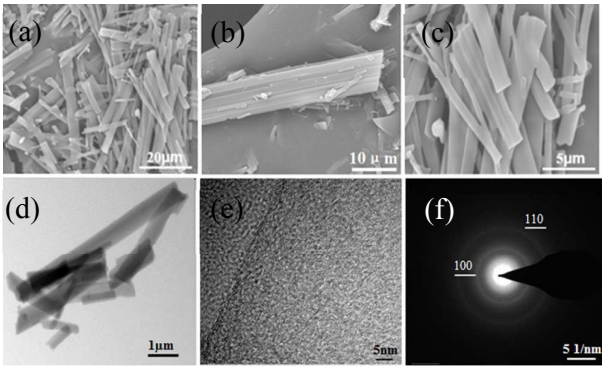

Fig. 1 SEM and TEM photos of the obtained poorly crystallized BN whiskers

The porous structure is further carried out using the N_2 adsorption-desorption isotherms as shown in Fig. 2. The isotherms are a characteristic of type I with type H4 loop according to the IUPAC nomenclature. However, the hysteresis loop is broad and steep. The isotherm and the broad hysteresis loop indicate that BN whiskers possess micropores and contain mesopores that are associated with capillary condensation. A surface area of 964.3 $m^2 \cdot g^{-1}$ was calculated using the Brunauer-Emmett-Teller (BET) model. For comparison, the BET characterization of BN whiskers with good crystallinity obtained at higher temperature [38] is also investigated as shown in Fig. S3 a and b. They show that the highly crystallized h-BN whiskers also possess micropores. The surface areas are calculated using the Brunauer-Emmett-Teller (BET) model to be 842.2$m^2 \cdot g^{-1}$.

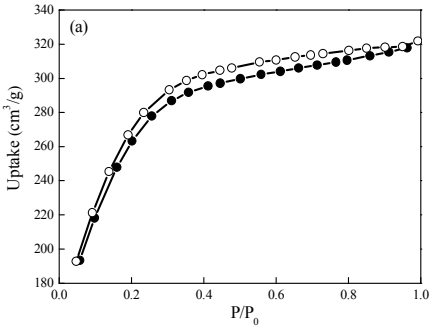

View Article Online
DOI: 10.1039/C5RA27234C

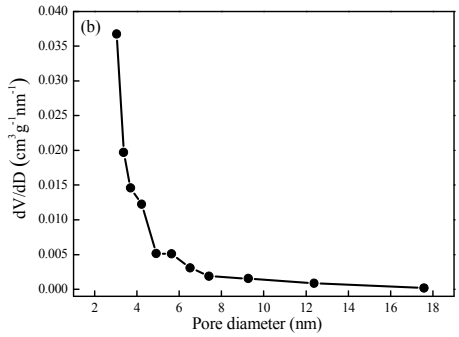

Fig. 2 (a) N_2 adsorption-desorption isotherms and (b) pore size distribution of the poorly crystallized BN whiskers

3.2 Electrochemical behaviour of h-BN whiskers electrode

By using a 0.005 mol·L^{-1} ferrocyanide and ferricyanide couple (1:1) as the redox probe and employing the BN whiskers as the working electrode, the charge-transfer rates at the solution/electrode interface in a 0.1 mol·L^{-1} KCl solution were measured. As shown in Fig. 3, the anodic and cathodic peaks associating with the oxidation and reduction of the ferricyanide-ferrocyanide couple respectively obviously appear at the BN-solution interface. It can be seen that anodic/cathodic peak are almost symmetrical, indicating that both ferrocyanide and ferricyanide are stable in solution and the electrode process is reversible. The anodic and cathodic peak current increases linearly with the square root of scan rates as shown in Fig. S4(a), exhibiting that the electrode reactions are diffusion controlled. Fig. S4(b), shows a set of Nyquist impedance spectra of the BN whisker electrode (a). For comparison, the Nyquist impedance spectra of the electrode without BN whisker (b) are also carried out. The Rct value for BN electrode (Rct=8.8Ω) is much smaller than that of electrode without BN (Rct=631.8Ω), indicating the faster charge-transfer rate at the BN electrode/solution interface.

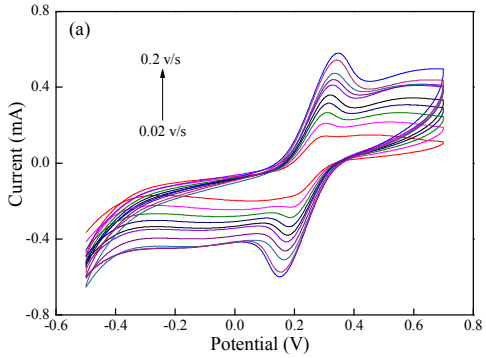

Fig. 3 Cyclic voltammograms of the poorly crystallized BN whiskers electrode at scan rates of 0.02, 0.04, 0.06, 0.08, 0.10, 0.12, 0.14, 0.16, 0.18,and 0.20 v/s in 0.10 M KCl containing 5 mM $[Fe(CN)_6]^{3-/4-}$

3.3 Electrochemical determination of nitrite

The electrochemical response of h-BN whiskers electrode to 1.0 m mol·L^{-1} nitrite in 0.1 mol·L^{-1} PB was investigated by cyclic voltammetry and the corresponding voltammogram was shown in Fig. 4 For comparison, the electrochemical behavior of BN whiskers with good crystallinity obtained at higher temperature [38] is also investigated. It can be seen that both almost overlap each other (curve a and b). For the bare electrode without BN whiskers (curve c), there is no existence of peak corresponding to the oxidation of nitrite. While for h-BN whiskers electrode, the peak potential shifts to +0.94v. This would be attributed to larger effective electrode surface.

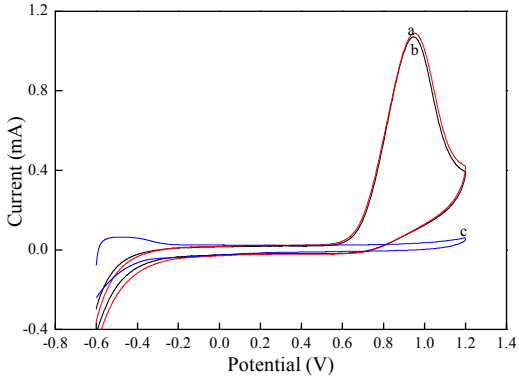

Fig. 4 CV curves of the poorly crystallized BN whiskers electrode (a), the highly crystallized BN whiskers electrode (b) and bare Ti electrode(c).

The influence of different pH values on the oxidation of NO_2^- at the h-BN whiskers electrode was studied by means of differential pulse voltammetry (DPV) in 0.10 mol·L^{-1} PB within the pH range of 2.0-8.0. As indicated in Fig. S4, the peak current corresponding to the oxidation of NO_2^- increaseds with the increase of the pH value until the pH value reached 3.0, and then begins to decrease obviously with the further increase of the pH value (Fig. S5). It is well known that NO_2^- is not stable in strong acidic media and can undergo the following reaction:[41]

$$2H^+ + 3NO_2^- \rightarrow 2NO + NO_3^- + H_2O$$

On the one hand, most nitrite anions are protonated in acidic solutions because the pKa of HNO_2 is 3.3.[42] Protonation was proven to be involved in the catalytic reaction process. Thus, in this case the electrochemically active species should be HNO_2 rather than NO_2.[43]When the pH is greater than 3.0, the electrocatalytic oxidation of nitrite will become more difficult due to the shortage of protons,[44] so the peak current will naturally decrease. And moreover, an -NH_2 group was converted into a non-nucleophilic amine (-NH^{3+}) in the case of the lower pH values, which made it easy to absorb NO_2^-.[45] Therefore, the PB of pH 3.0 was selected as the optimum electrolyte in the electrochemical detection of nitrite.

The influence of different scan rates on the oxidation behavior of NO_2^- at the h-BN whiskers electrode was investigated using the CV method. Fig. 5(a) indicates that the peak currents increase continuously with the increase of the scan rate in the range of 0.03–0.17v/s. Moreover, there is a linear relationship between the peak current (Ip) and the scan rate ($v^{1/2}$) (Fig. 5(b)), indicating that the oxidation process of NO_2^- is a typical diffusion controlled process. The fitted regression equation can be expressed as follows:

$$Ip(A) = 2.2310^{-3}v^{1/2} + 7.59\times10^{-5} (R^2=0.995)$$

The correlation coefficient is 0.995, indicating that the oxidation of nitrite on h-BN whiskers is a typical diffusion-control process. In addition, it is observed that the oxidation peak potentials (E_{pa}) shifts to more positive potentials with the increase of the scan rate, leading to a linear relationship between E_{pa} and logv(Fig. 5(c)). The regression equation is given below:

$$E_{pa} = 1.19 + 0.146\log v \text{ (v/s)} \ (R^2=0.993)$$

For an irreversible process, the E_{pa} can be represented by the following equation:[45]

View Article Online
DOI: 10.1039/C5RA27234C

$$E_{pa} = E^{\theta} + (\frac{RT}{\alpha nF})\ln(\frac{RTK^{\theta}}{\alpha nF}) + (\frac{RT}{\alpha nF})\ln v$$

where α is the electron transfer coefficient, n is the number of transfer electron, R, T and F have their usual meanings. Thus, αn was calculated to be 0.455. Generally, α is assumed to be 0.5 in a totally irreversible electrode process. Therefore, the number of transfer electron (n) in electro-oxidation of nitrite was about 1, which was in agreement with previous literature reports.[46]

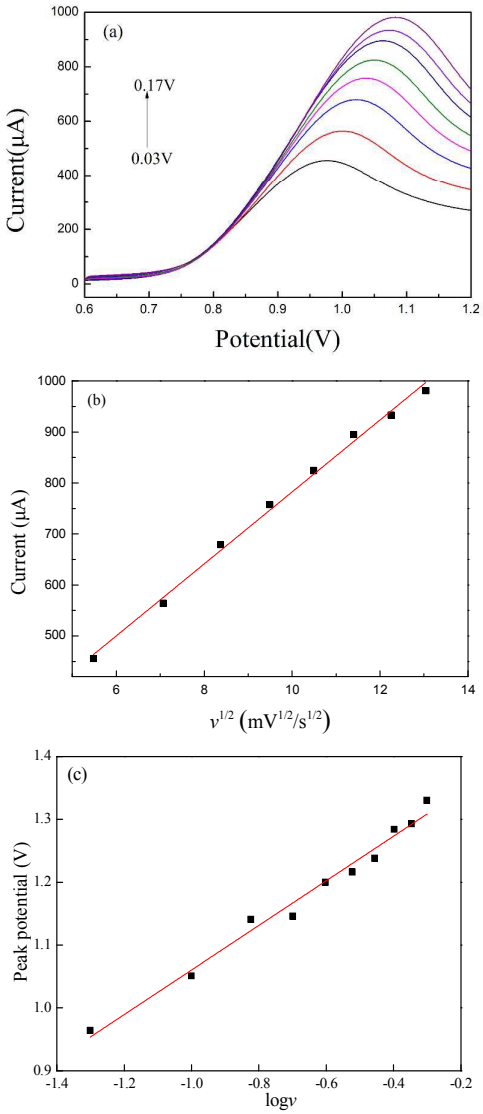

Fig. 5 (a) CVs of the poorly crystallized BN whiskers electrode in 0.10 M PB (pH 3.0) containing 0.10 mM NO_2^- at different scan rates. (b) The linear dependence of Ipon $v^{1/2}$. (c) The linear dependence of E_{pa} on logv.

A typical current-time response curve for the successive addition of NO_2^- to stirred 0.10 mol·L^{-1} PB (PH 3.0) at the applied potential of +0.8V is shown in Fig. 6. A well-defined and fast amperometric response was observed under the above-mentioned condition. For the low crystallinity BN whisker electrode, the detection range of NO_2^- is from 10 to 400 μmol·L^{-1} and 400 to 6300 μmol·L^{-1}. Based on the calibration curve for the steady state current versus NO_2^- concentration (Fig. S6(a) and (b)), the fitting regression equation is given as follows:

Ip(μA)=10.77+0.198C(μmol·L^{-1})(R^2=0.992) (10 to 400 μmol·L^{-1})

and

Ip(μA)=117.47+0.043C(μmol·L^{-1})(R^2=0.994) (400 to 6300 μmol·L^{-1})

The limit of detection is 0.089 and 0.412μmol·L^{-1} (S/N=3) respectively.

The parallel experiments on the electrochemical sensing evaluations for the h-BN whiskers with high crystallization are also carried out. In an analogous way, Fig.6c and d is the current response to low concentrations of $NaNO_2$ on the highly crystallized BN whiskers. A well-defined and fast amperometric response was also observed under the above-mentioned condition. The detection range of NO_2^- is 20 to 400 μmol·L^{-1} and 400 to 5200 μmol·L^{-1}. Based on the calibration curve for the steady state current versus NO_2^- concentration (Fig. S6(c) and (d)), the fitting regression equation is also given as follows:

Ip(μA)=8.19+0.175C(μmol·L^{-1})(R^2=0.997) (20 to 400 μmol·L^{-1})

and

Ip(μA)=95.26+0.037C(μmol·L^{-1})(R^2=0.991) (400 to 5200 μmol·L^{-1})

The limit of detection is 0.101 and 0.478μmol·L^{-1} (S/N=3) respectively.

Compared with the detection limitation of the electrodes for electrochemical nitrite detection (Table 1), h-BN whiskers electrode exhibits relatively higher sensitivity in the range from 10 to 6300 μmol·L^{-1} and 20 to 5200 μmol·L^{-1}.For instance, Au-G-PANI/GC electrode(0.01 mmol·L^{-1}, 0.1-205.8 μmol·L^{-1}), nanometer-sized gold colloid/ethylenediamine/PGCE electrode(45 mmol·L^{-1}, 130 to 44000 μmol·L^{-1}), Hb/Au modified electrode (0.06 mmol·L^{-1}, 0.4-14.8 μmol·L^{-1}), GR/PPy/CS/GCE electrode (0.1 mmol·L^{-1}, 0.5-722 μmol·L^{-1}), nafion-Au/P3MT/GCE electrode (2.3 mmol·L^{-1}, 10-1000 μmol·L^{-1}), Au@Fe_3O_4/Cys/GCE electrode (0.82 mmol·L^{-1}, 3.6-10000 μmol·L^{-1}) and Nafion /SLGnP–TPA–Mb/GCE electrode (10 mmol·L^{-1}, 50-250 μmol·L^{-1}). The enhanced electrochemical behavior can be attributed to the combination of the excellent electrocatalytic properties of h-BN whiskers and large surface area.

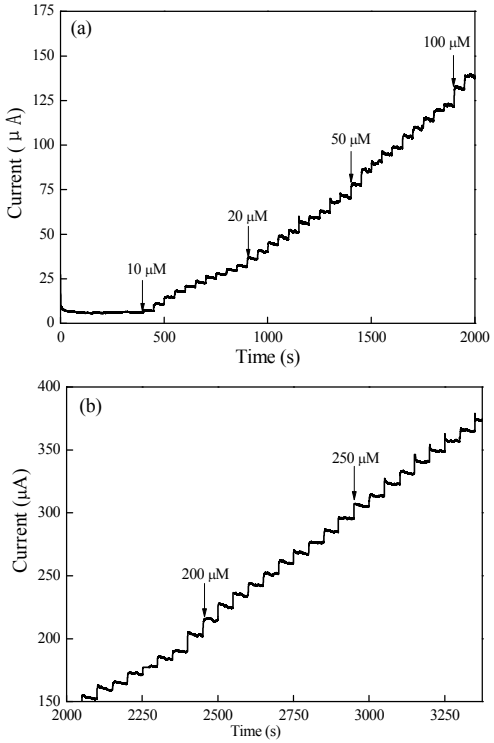

View Article Online
DOI: 10.1039/C5RA27234C

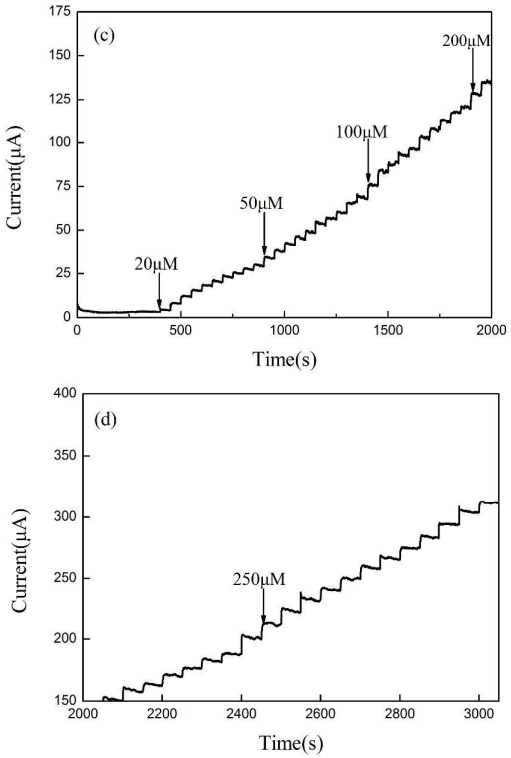

Fig.6 The current response to low concentrations of $NaNO_2$ on the poorly (a, b) and highly crystallized (c, d) BN whiskers. Supporting electrolyte: 0.10 mol·L-1 PB; applied potential:+0.80V

From above experimental results, the good performance of BN whiskers electrode toward nitrite is mainly attributed to their microstructure, i.e. the large surface area and highly porous nature. While from the viewpoint of fabrication process of BN, BN whiskers with low crystallinity can be prepared at relatively lower temperature (1073-1273K) compared with that for BN whiskers with high crystallinity (1873K). Therefore in this work, BN whiskers with low crystallinity are selected as electrode for electrochemical detection of nitrite.

Table 1 Performance comparison of the NO_2^- detection between h-BN whiskers electrode and other electrode.

Electrode	Detectin limit (m mol·L^{-1})	Linear range (m mol·L^{-1})	R^2	references
Nafion/SLGnP-TPA-Mb/GCE	10	50-250	0.992	47
Au@Fe_3O_4Cys/GCE	0.82	3.6-10000	0.998	48
NafinoAu/P3MT/GCE	2.30	10-1000		43
GR/PPy/CS/GCE	0.10	0.5-722	0.996	49
Hb/Aumodified electrode	0.06	0.4-14.8	0.998	50
Nanometer-sized goldcolloid/ethylene diamine/PGCE	45	130-44000	0.998	51
Low crystallinity h-BN whiskers electrode	8.9×10^{-5} 4.1×10^{-4}	0.01-0.4 0.4-6.3	0.992 0.994	This work
High crystallinity h-BN whiskers electrode	1.01×10^{-4} 4.78×10^{-4}	0.02-0.4 0.4-5.2	0.997 0.991	This work

To investigate the possible use of the proposed method, the experiments were studied in tapwater to determine nitrite by DPV using the standard addition method. The results are shown in Table 2, and the recoveries ranged between 94.8% and 97.1%. Therefore, the developed sensor can be preliminarily applied to determine nitrite in environmental samples.

Table 2 Determination of nitrite at various concentrations in tap water

Sample	Analyte	Added (μM)	Found (μM)	Recovery (%)
1	NO_2^-	100	94.8	94.8
2	NO_2^-	200	190.3	95.2
3	NO_2^-	500	480.0	96.0
4	NO_2^-	800	764.2	95.5
5	NO_2^-	1000	970.8	97.1

The reproducibility of h-BN whiskers electrode was investigated in 0.10 mol·L^{-1} PB (pH 3.0) containing 1 m mol·L^{-1} NO_2^- by means of the DPV method (Fig. S7). The reproducibility of the developed method was evaluated using four different h-BN whiskers electrode in 0.10 mol·L^{-1} PB(pH 3.0) with 1 m mol·L^{-1} NO_2^-, the resulting RSD of peak current was about 5.31% and RSD of peak potential was 0.87%. Furthermore, the stability of the h-BN whiskers electrode was investigated by measuring the current response after the h-BN whiskers electrode was stored at 298K for a month. The current response still retained more than 92% of the initial response. It is evident that the h-BN whiskers electrode presents good reproducibility and stability for NO_2^- determination.
The possible interference for the nitrite detection was investigated by adding some inorganic ions, which may coexist with nitrite in real samples, into the pH 3.0 PB solution. As shown in Fig. 7, the h-BN whiskers electrode exhibits well amperometric response towards each addition of 5 μmol·L^{-1} nitrite (a). However, there was no significant response observed for each 1000-fold excessive addition of $CaCl_2$ (b), Na_2SO_4 (c), NaCl (d), KCl (e). Interestingly, every addition of nitrite (a) produced a noteworthy response, which reveals excellent selectivity of the proposed sensor. The results clearly demonstrate that nitrite can be selectively detected by h-BN whiskers electrode even when there are large quantities of other common species.

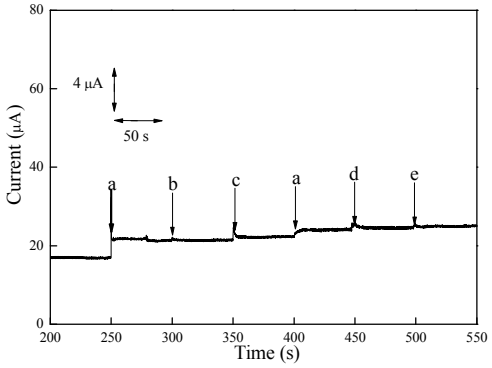

Fig. 7 The amperometric response at the h-BN whiskers electrode for 5 μM of nitrite(a) in the presence of 1000-fold:$CaCl_2$ (b), Na_2SO_4

View Article Online
DOI: 10.1039/C5RA27234C

(c), NaCl (d), KCl(e)

The excellent electrochemical behavior of BN whiskers for nitrite may be attributed that BN whiskers possess high density defects and micro/mesopore in structure, which provide large surface area and void volume. These features would offer numerous active sites for the enhanced adsorption of nitrite onto the surface as shown in Fig. 8. The highly porous nature of BN whiskers allowed fast electron transfer due to their high-energy adsorption sites and thus leads to high sensitivity and selectivity. In addition, the large surface area of BN whiskers with micropores and mesopores enabled the highly sensitive detection of nitrite.

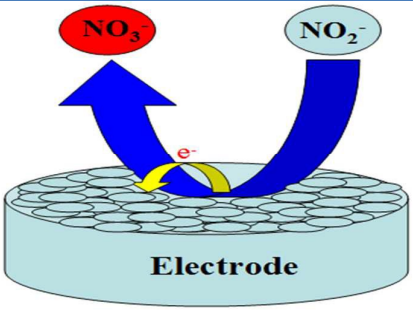

Fig. 8 The proposed mechanism of h-BN whiskers nitrite sensor in water sample

Conclusions

Hexagonal boron nitride whiskers were successfully fabricated via polymeric precursor method, which offered a simple and versatile method to synthesize the long ceramic whiskers. The obtained BN whiskers were polycrystalline and the morphology was uniform with 0.5-3μm in diameter and 200-500 mm in length. Moreover, a nitrite electrochemical sensor based on the BN whiskers was fabricated. The CVs of the h-BN whiskers electrode show an obvious oxidation peak and significantly enhanced peak currents for the oxidation reactions of NO_2^-, which are due to the fact that h-BN whiskers have the advantages of the large surface area, high energy adsorption sites and highly porous nature. The h-BN whiskers electrode also presents much higher sensitivity in a wide linear range. Therefore BN whiskers may be a promising electrochemical sensor material for the high sensitivity detection of certain environmental pollutants in the near future.

Acknowledgements

The authors express their appreciation to National Nature Science Foundation of China (No. 51572019 and 51474141) and Program for Yangtze Scholars and Innovative Research Team in University (IRT1207) for financial support. The authors also appreciate the National Science Fund for Excellecnt Young Scholars of China (No. 51522402) for financial support.

Notes and references

1 B. R. Kozub, N. V. Rees and R. G. Compton, Sensor Actuat. B, 2010, **143**, 539-546.
2 W. Lijinsky, E. Conrad and R. V. D. Bogart, Nature,1972, **239**, 165-167.
3 S. S. Mirvish, Cancer Lett, 1995, **93**, 17–48.
4 T. Zhanga, H. Fan and Q. Jin, Talanta, 2010, **81**, 95–99.
5 X. H. Tu, B. D. Xiao, J. Xiong and X. D. Chen, Talanta, 2010, 82, 976–983.
6 G. H. Chen, D. X. Yuan, Y. M. Huang, M. Zhang and M. Bergman, Anal. Chim. Acta, 2008, **620**, 82–88.
7 M. Zhang, Z. Zhang, D. X. Yuan, S. C. Feng and B. M. Liu, Talanta, 2011, **84**, 443–450.
8 C. Y. Lin, A. Balamurugan, Y. H. Lai and K. C. Ho, Talanta, 2010, **82**, 905–911.
9 P. Li, Y. Ding, A. Wang, L. Zhou, S. Wei, Y. Zhou and T. Lu, ACS Appl. Mater. Interfaces, 2013, **5**, 2255–2260.
10 L. Zhoua, J. P. Wanga, L. Gaia, D. Li and Y. B. Li, Sensors and Actuators, B, 2013, **181**, 65–70.
11 V. Mani, A. P. Periasamy and S. M.Chen, Electrochem. Commun, 2012, **17**, 75–78.
12 D. Zhang, Y. Fang, Z. Miao, M. Ma, X. Du, S. Takahashi and Q. Chen, Electrochim. Acta, 2013, **107**, 656–663.
13 L. Cui, T. Pu, Y. Liu and X. He, Electrochim. Acta, 2013, **88**, 559–564.
14 S. J. Li, G. Y. Zhao, R. X. Zhang, Y. L. Hou, L. Liu and H. Pang, Microchim. Acta, 2013, **180**, 821–827.
15 V. Mani, T. Y. Wu and S. M. Chen, J Solid State Electrochem, 2014, **18**, 1015–1023.
16 X. R. Li, F. Y. Kong, J. Liu, T. M. Liang, J. J. Xu and H. Y. Chen, Adv. Funct. Mater, 2012, **22**, 1981–1988.
17 V. Mani, B. Dinesh, S. M. Chen and R. Saraswathi, Biosens and Bioelectron, 2014, **53**, 420–427.
18 D. Ye, L. Luo, Y. Ding, Q. Chen and X. Liu, Analyst, 2011, **136**, 4563–4569.
19 A. Afkhami, F. S. Felehgari, T. Madrakian and H. Ghaedi, Biosensors and Bioelectronics, 2014, **51**, 379–385.
20 Y. Zhanga, Y. Zhao, S. Yuan, H. Wanga and C. He, Sensors and Actuators B, 2013, **185**, 602–607.
21 M. L. Guo, J. H. Chen, J. Li, B. Tao and S. Z. Yao, Analytica Chimica Acta, 2005, **532**, 71–77.
22 P. Miao, M. Shen, L. M. Ning, G. F. Chen and Y. M. Yin, Analytical and Bioanalytical Chemistry, 2011, **399** ,2407–2411.
23 G. R. Xu, G. F. Xu, M. L. Xu, Z. Q. Zhang, Y. Tian, H. N. Cho and W. Y. Lee, Bulletin of the Korean Chemical Society, 2012, **33**, 415–419.
24 B. Sljukic, C. E. Banks, A. Crossley and R. G. Compton, Electroanalysis, 2007, **19**,79–84.
25 T. Yao, S. Musha and Anal. Chim, Acta, 1979, 110, 203–209.
26 K. Ravichandran and R. P. Baldwin, J, Electroanal. Chem, 1981, **126**, 293–300.
27 J. Economy and R. V. Anderson, Journal of Polymer Science Part C, 1967, **19**, 283–297.
28 R. T. Paine and C. K. Narula, Chemical Reviews, 1990, 90, 73–91.
29 K. Watanabe T. Taniguchi and H. Kanda, Nature Materials, 2004, **3**, 404–409.
30 J. A. Perdigon-Melon, A. Auroux, C. Guimon, B. Bonnetot and B. N. Micrometric, Journal of Solid State Chemistry, 2004, **177**, 609–615.
31 L. X. Lin, Y. Zheng, Y. Zheng and K. M. Wei, Materials Letters, 2007, **61**, 1735–1737.
32 N. G. Chopra, R. J. Luyken, K. Cherrey, V. H. Crespi, M. L. Cohen, S. G. Louie and A. Zettl, Science, 1995, **269**, 966–967.
33 D. Golberg, Y. Bando, M. Eremets, K. Takamura, K. Kurashima and H. Yusa, Appl. Phys.Lett, 1996, **69**, 2045–2047.
34 M. Terauchi, M. Tanaka, H. Matsuda, M. Takeda and K. Kimura, J. Electron Microsc, 1997, **1**, 75–78.

View Article Online
DOI: 10.1039/C5RA27234C

35 O. R. Lourie, C. R. Jones, B. M. Bartlett, P. C. Gibbons, R. S. Ruoff and W. E. Buhro, Chem. Mater, 2000, **12**,1808–1810.
36 Y. Cheng, X. W. Yin, Y. S. Liu, S. W. Li, L. F. Cheng and L. T. Zhang, Surf. Coat. Technol, 2010, **204**, 2797–2802.
37 F. Ye, L. Zhang, Y. Liu, S. Li, M. Su, X.Yin and L. Cheng, Progress in Natural Science: Materials International, 2012, **22**, 433-439.
38 X. Hou, Z. Yu, K C. Chou. Ceramics International, 2013, **39**, 6427-6431.
39 G. Lian, X. Zhang, M. Tan, S. Zhang, D. Cui and Q. Wang, J. Mater. Chem, 2011, **21**, 9201-9207.
40 Y. C. Zhu, Y. Bando, L. W. Yin and D. Golberg, Chemistry-A European Journal, 2004, **10**, 3667-3672.
41 O. Brylev, M. Sarrazin, L. Rou´e and D. B´elang´er, Electrochim. Acta, 2007, **52**, 6237–6247.
42 G. Milczarek, J. Electroanal. Chem., 2007, 610, 199–204.
43 X. Huang, Y. X. Li, Y. L. Chen and L. Wang, Sens. Actuators, B, 2008, **134**, 780–786.
44 L. Y. Jiang, R. X. Wang, X. M. Li, L. P. Jiang and G. H. Lu, Electrochem. Commun., 2005, **7**, 597–601.
45 E. Laviron and L. Roullier, Electroanal. Chem., 1980, **115**, 65–74.
46 B. R. Kozub, N. V. Rees and R. G. Compton, Sensors and Actuators B, 2010, **143**, 539–546.
47 R. Yue, Q. Lu and Y. K. Zhou, Biosens. Bioelectron., 2011, **26**, 4436–4441.
48 C. M. Yu, J. W. Guo and H. Y. Gu, Electroanalysis, 2010, **22**, 1005–1011.
49 D. X. Ye, L. Q. Luo, Y. P. Ding, Q. Chen and X. Liu, Analyst, 2011, **136**, 4563–4569.
50 B. Q. Yuan, C. Y. Xu, L. Liu, Y. F. Shi, S. J. Li, R. C. Zhang and D. J. Zhang, Sens. Actuators, B, 2014, **198**, 55–61.
51 A. Abbas, S. F. Farzaneh, M. Tayyebeh and G. Hamed, Biosens. Bioelectron., 2014, **51**, 379–385.